Original Research *Highlight article*

Differential expression and alternative splicing of transcripts in orbital adipose/connective tissue of thyroid-associated ophthalmopathy

Lianqun Wu[1,2,3,*], Yu Liang[1,2,3,*], Nan Song[4,*], Xiying Wang[1,2,3], Chao Jiang[1,2,3], Xinxin Chen[5], Bing Qin[6], Xiantao Sun[7], Guohua Liu[8] and Chen Zhao[1,2,3]

[1]Eye Institute and Department of Ophthalmology, Eye & ENT Hospital, Fudan University, Shanghai 200031, China; [2]NHC Key Laboratory of Myopia (Fudan University), Key Laboratory of Myopia, Chinese Academy of Medical Sciences, Shanghai 200031, China; [3]Shanghai Key Laboratory of Visual Impairment and Restoration, Shanghai 200031, China; [4]Department of Facial Plastic and Reconstructive Surgery, Eye & ENT Hospital, Fudan University, Shanghai 200031, China; [5]Department of Ophthalmology, Changzheng Hospital, Second Military Medical University, Shanghai 20003, China; [6]Department of Ophthalmology, Suqian First Hospital, Suqian 223800, China; [7]Department of Ophthalmology, Children's Hospital Affiliated of Zhengzhou University, Zhengzhou 450053, China; [8]Department of Ophthalmology, Qilu Children's Hospital of Shandong University, Jinan 250022, China

Corresponding author: Chen Zhao. Email: dr_zhaochen@fudan.edu.cn

*These authors contributed equally to this work.

Impact statement

Thyroid-associated ophthalmopathy (TAO) is a common ocular autoimmue complication of thyroid dysfunction, but its mechanism is poorly understood. To our best knowledge, we are the first to sequence total RNA from orbital adipose/connective tissue samples to analyze alternative splicing pattern in TAO. We found the prevalence of alternative splicing in transcriptome of TAO, which significantly influences immune response, extracellular matrix remodeling, and adipogenesis in orbit of patients. This manuscript shed light on the important role of alternative splicing mechanism in modulating the development of TAO, and it will also provide contribution to current understanding of TAO as well as the potential treatment strategy against autoimmune disease for further studies.

Abstract

Thyroid-associated ophthalmopathy is a typical autoimmune disease of orbital tissues. Alternative splicing significantly influences many diseases progression, including cancer, age-related macular degeneration, and multiple sclerosis, by modulating the expression of transcripts. However, its role in thyroid-associated ophthalmopathy is still unclear. In this study, differential expression transcripts and differential alternative splicing genes in orbital adipose/connective tissues of thyroid-associated ophthalmopathy patients were detected using RNA sequencing, Cuffdiff, and replicate multivariate analysis of transcript splicing. Three thousand ninety six differential expression transcripts and 2355 differential alternative splicing genes were screened out, while functional enrichment analysis indicated that differential expression transcript and differential alternative splicing genes were associated with immune modulation, extracellular matrix remodeling, and adipogenesis. The expression of the *SORBS1*, *SEPT2*, *COL12A1*, and *VCAN* gene transcripts was verified by qRT-PCR. In conclusion, prevalent alternative splicing is involved in the disease development in thyroid-associated ophthalmopathy. More attention should be paid to the mechanism of alternative splicing to explore more potential therapeutic targets in thyroid-associated ophthalmopathy.

Keywords: Thyroid-associated ophthalmopathy, alternative splicing, rMATS, adipogenesis, adipose/connective tissue

Experimental Biology and Medicine **2021; 246: 1990–2006. DOI: 10.1177/15353702211017292**

Introduction

Thyroid-associated ophthalmopathy (TAO) is a common ocular manifestation involved in thyroid dysfunction, which occurs most frequently in patients with Graves' disease.[1] As an autoimmune disease, TAO is characterized by an abnormal autoimmune response against antigens, such as thyroid-stimulating hormone receptor (TSHR), calsequestrin, and collagen XIII, shared by the thyroid and the orbit.[2,3] In the orbit, infiltrating T cells mainly provoke the activation of orbital fibroblasts and lead to extracellular matrix (ECM) remodeling.[4,5] Orbital fibroblasts (OFs) are

the critical effectors in TAO and are divided into two populations according to the expression of surface glycoprotein Thy-1. Thy-1-positive cells are prone to differentiating into myofibroblasts, whereas Thy-1-negative cells mainly undergo differentiation into adipocytes in response to elevated levels of peroxisome proliferator-activated receptor gamma (PPARγ), which is responsible for an increased volume of orbital adipose/connective tissue (OACT).[5,6] Merging studies have revealed the close association of OFs with adipogenesis and TAO. For example, the expression of TSHR is increased during adipogenesis in TAO patients, while insulin-like growth factor-1 (IGF-1) boosts stromal cells to significantly proliferate in TAO periorbital adipose tissues.[7,8] However, the modulatory mechanism underlying the activation of fibroblasts and adipogenesis in adipose/connective tissues in TAO has yet to be discovered.

Accumulating epidemiological evidence demonstrates the genetic etiology of TAO. More than 50 genes that contribute to TAO have been identified, including *TSHR*, *CTLA-4*, *CD40*, *HLA-DR*, *HLA-DQ*, and *TNF-α*.[5,9] Moreover, differentially expressed genes associated with the cell cycle, pathways of ribosomes, and retinol metabolism have been identified as critical regulators of TAO,[10] providing new insights into the pathogenesis and therapeutic targets of the disease. The important role of post-transcriptional regulation in orbitopathy has recently been confirmed. In OFs in TAO, miR-21 is overexpressed and regulates orbital muscle fibrosis.[11] Our previous study revealed the potential regulatory function of the circRNA_14940/CCND1/Wnt signaling pathway in TAO using high-throughput RNA sequencing.[12]

Alternative splicing (AS) is a regulated process that enables a single messenger RNA (mRNA) precursor (pre-mRNA) to produce different functional proteins by rearranging the pattern of intron and exon elements, thereby significantly increasing the complexity of gene expression.[13] AS has been proven to play a vital role in many biological processes over the entire life span and in the development of the brain, testes, and immune system.[13] Furthermore, AS-related factors, such as Sam68, SRSF10, and SRp40, participate in adipogenesis processes and regulate the AS events of the mammalian target of rapamycin (mTOR), Lipin1, and PPARγ.[14] The activation and differentiation of human monocytes under stimulation is also modulated by specific splicing events.[15] Merging evidence also reveals that alternative splicing is associated with the pathogenesis of macular and autoimmune diseases, such as age-related macular disease, multiple sclerosis, and cancer.[16–18] However, the knowledge of the relationship between AS and TAO remains to be expanded.

In this study, to explore the potential relationship between AS and TAO, differential expression transcripts (DETs) and differential alternative splicing (DAS) genes were identified based on high-throughput RNA sequencing data of tissues from TAO and control subjects, using replicate multivariate analysis of transcript splicing (rMATS). Then, Gene Ontology (GO) and Kyoto Encyclopedia of Genes and Genomes (KEGG) pathway analysis were obtained to screen out significantly enriched functions through the DAVID database. Furthermore, quantitative real-time polymerase chain reaction (qRT-PCR) was performed to validate DET and DAS genes.

Materials and methods

Patients and tissue samples

All patients included in this study were diagnosed with TAO based on the Bartley criteria and had normal thyroid functions after treatment with antithyroid drugs.[19] The following patients were excluded: (i) patients with other ocular or systemic inflammatory or autoimmune diseases, (ii) patients who had undergone radioiodine therapy or thyroid operations, and (iii) patients who had been treated with anti-inflammatory and/or immunosuppressive drugs (e.g. steroids) within six months prior to the study. Six TAO patients were screened out, and all of these cases were recognized as inactive TAO with a clinical activity score (CAS) of less than three for at least six months.[20] Additionally, six individuals who had not been diagnosed with thyroid or orbital diseases or any inflammatory/autoimmune diseases participated in the study as controls. OACT samples of TAO patients were collected from tissue removed during orbital decompression surgery. Besides, tissues of control individuals obtained in plastic surgery were collected as control samples.

Ethical approval

This study was approved by the Ethics Committee of Changzheng Hospital, Second Military Medical University. All patients signed informed consent forms based on a full understanding of the study's aims and procedures before being enrolled. The research protocol complied with the provisions of the Declaration of Helsinki.

RNA isolation and sequencing

Total RNA was isolated using TRIzol reagent (Invitrogen, Carlsbad, CA, USA) according to the manufacturer's protocol. The integrity of RNA was evaluated using an Agilent 2100 Bioanalyzer (Agilent Technologies, Palo Alto, CA, USA). Its quality and quantity were assessed using a Nanodrop 2000 (Thermo Scientific, Waltham, MA, USA).

Using a TruSeq Stranded Total RNA kit and Ribo-Zero Gold treatment (Illumina, San Diego, CA, USA), strand-specific RNA sequencing libraries were established after ribosomal RNA was depleted according to the manufacturer's protocol. For each sample, extracted RNA was used for double stranded cDNA synthesis, and then was purified and adenylated and ligated with adapters at the 3′ ends. The DNA fragments were enriched by PCR with 14 cycles and the main peak of the library was 350 bp. After evaluating the library quality using an Agilent 2100 Bioanalyzer (Agilent Technologies), high-throughput RNA sequencing was performed using a HiSeq 2500 System (Illumina). The RNA sequencing data of each sample was 97.96 M to 99.79 M reads.

Sequence assembly and analysis

The quality of raw reads was assessed using Trimmomatic.[21] Adapters, low-quality bases, and reads

were filtered out. The remaining clean reads were aligned with the human genome (GRCh38.p12) for assembly using HISAT2.[22] Sequence segments were spliced and annotated, and the transcript expression counts were calculated using the htseq-count script.[23] Gene expression was quantified with Cufflinks with fragments per kilobase of exon per million mapped reads (FPKM),[24] and the read counts were normalized with DESeq.[25] PCA of samples was exhibited based on the expression of the transcripts.

AS allows one gene to produce multiple mRNA transcripts that may be translated into different proteins. Based on the mapping results (in BAM format), we detected the presence of AS events in the samples using rMATS.[26] Through rMATS, alternative splicing events that corresponded to known alternative splicing patterns was automatically detected and analyzed.

DET and DAS analysis

DETs were screened out based on the FPKM values according to the criteria of $\log2|\text{fold change}| > 1$ and $P < 0.05$. To identify homogeneous groups of all samples, pheatmap package in R was used to make hierarchical clustering analysis according to the expression levels of the transcripts.[27]

DAS genes in TAO patients and controls were identified using rMATS.[26] Five main alternative splicing events, A3SS, A5SS, MXE, RI, and SE, were analyzed. The DAS genes were calculated with a threshold of $|\text{IncLevelDifference}| > 0.01$ and FDR-adjusted $P < 0.05$.

Functional enrichment analysis

DET and DAS genes were selected and subjected to Gene Ontology and Kyoto Encyclopedia of Genes and Genomes pathway analysis. In terms of the GO analysis, the related genes were annotated according to BP, CC, or MF. For KEGG analysis, the differentially enriched pathways were ranked by the enrichment scores.

Quantitative real-time PCR

Total RNA of orbital tissue from two groups was isolated using TRIzol reagent (Invitrogen), and was reverse-transcribed into complementary DNA using a HiScript II Q RT SuperMix IIa Kit (Vazyme Biotech, Shanghai, China). Quantitative RT-PCR was performed using a ChamQ SYBR qPCR Master Mix Kit (Vazyme) on a GeneAmp PCR System 9700 (Applied Biosystems, Foster City, CA, USA). All samples were normalized to internal β-actin controls, and the relative expression levels of target genes were calculated using the $2^{-\Delta\Delta Ct}$ method. The primer sequences of all target genes are shown in Table S1.

Results

DETs in OACT samples of TAO patients

In total, 113,095 genes were identified in RNA sequencing profile derived from samples of TAO and control group. The unique mapped reads were assembled into transcripts using Cufflinks, and the expression of mRNAs was quantified by the FPKM values. The box plot of the FPKM values of mRNAs revealed no abnormal expression in three samples of each group (Figure 1(a)). Principal component analysis (PCA) revealed a clear separation between the samples of the two groups (Figure 1(b)). With a threshold of $\log2|\text{fold change}| > 1$ and a P value of <0.05, a total of 3096 DETs were screened, consisting of 1460 upregulated genes and 1636 downregulated transcripts (Figure 1(c)). Hierarchical clustering analysis showed two distinct separate clusters, suggesting that TAO and control samples could evidently be discriminated according to the expression of the 3096 DE genes (Figure 1(d)).

DAS gene analysis

To investigate potential AS in TAO patients, five main types of AS events, including alternative 3′ splice sites (A3SS), alternative 5′ splice sites (A5SS), mutually exclusive exons (MXE), retained intron (RI), and skipped exon (SE), were analyzed using rMATS (Figure 2(a)). AS events were detected in 12,021 genes. A3SS events occurred in 4298 genes, A5SS events occurred in 3593 genes, MXE events occurred in 3193 genes, RI events occurred in 1196 genes, and SE events occurred in 11,767 genes (Figure 2(b)). Within them, 130 overlapping genes were regulated by all five main AS events. Furthermore, 2533 DAS genes were identified in TAO and control groups, with a threshold of $|\text{IncLevelDifference}| > 0.01$ and a false recovery rate (FDR)-adjusted P value of <0.05 (Figure 2(c)). The numbers of A3SS, A5SS, MXE, RI, and SE events were 503, 386, 203, 140, and 2347, respectively. SE was the most prevalent AS event in TAO patients, whereas RI was the least prevalent.

Enrichment analysis of DET genes

Aimed at investigating the functions of DET genes, the functional enrichment analysis was exhibited based on GO annotation and KEGG pathway databases. The top 30 most significant GO terms of upregulated and downregulated DET genes were identified (Figures 3 and 4). The upregulated mRNAs of TAO samples were mainly related to the T cell antigen processing and presentation (biological process [BP]) and prostaglandin F receptor activity (molecular function [MF]), which were involved in the immune response and inflammation in TAO, as well as microtubule anchoring (BP), proteinaceous extracellular matrix (cellular component [CC]), kinetochore microtubule (CC), and microtubule plus-end binding (MF), which were associated with fibroblast activation (Figure 3, Table 1). The downregulated mRNAs were mostly connected with to cell adhesion (BP), the collagen catabolic process (BP), collagen type XII trimer (CC), extracellular matrix (CC), integrin binding (MF), and extracellular matrix structural constituent conferring tensile strength (MF), which were mainly associated with ECM remodeling and the interaction between immune cells and the ECM (Figure 4, Table 1).

The top 20 enrichment KEGG pathways were listed (Figures 5 and 6). The pathways associated with upregulated mRNAs included the PPAR signaling pathway, the transforming growth factor beta (TGF-β) signaling pathway, the insulin signaling pathway, the regulation of the actin cytoskeleton, and the interleukin 17 (IL-17) signaling

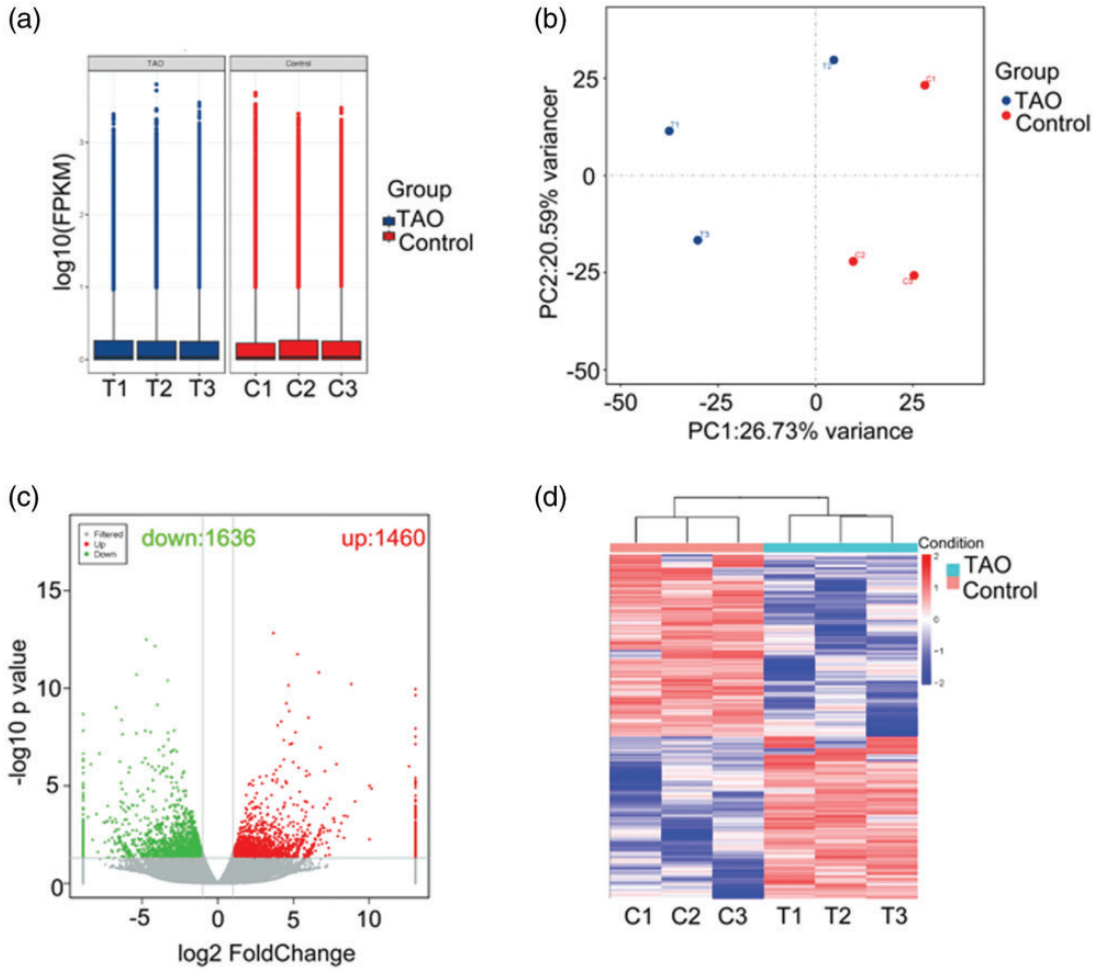

Figure 1. Qualification and analysis of identified genes from RNA sequencing data. (a) Box plot of FPKM values of transcripts in TAO and control groups. (b) Scatter plot of the PCA analysis for each sample on the first (PC1) and second principal components (PC2). (c) Volcano plot of differential expression transcripts based on a threshold of log2|fold change| > 1 and $P < 0.05$. (d) Heatmap of hierarchical clustering analysis for all samples based on the expression of genes. (A color version of this figure is available in the online journal.)

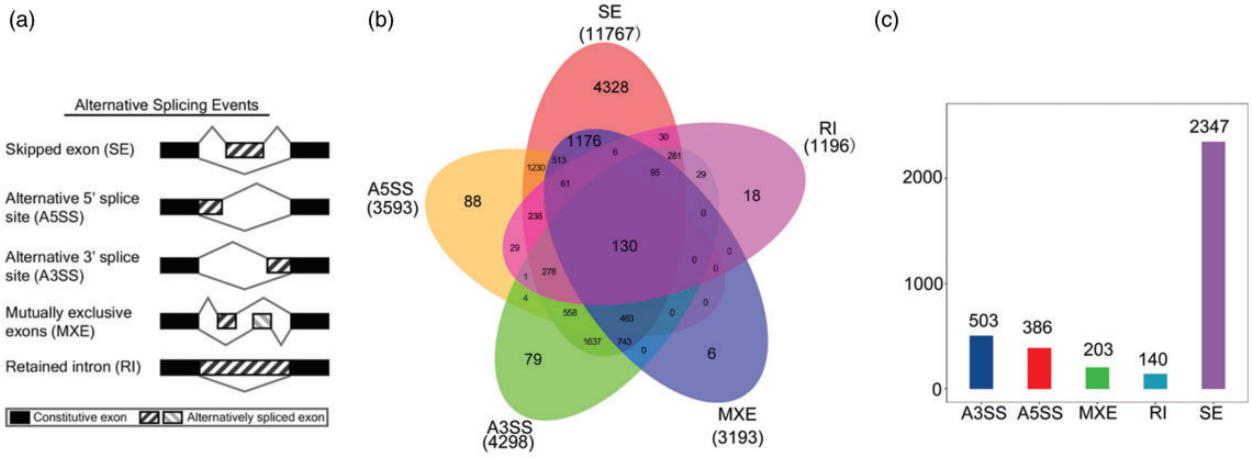

Figure 2. Analysis of differential alternative splicing (AS) genes and distribution of the five main AS events. (a) Schematic diagrams of the mechanisms of the five main AS events. (b) Venn diagram of the detected genes undergoing the five AS events and overlap of these genes. (c) Distribution of differential AS events based on a threshold of |IncLevelDifference| > 0.01 and FDR-adjusted $P < 0.05$. (A color version of this figure is available in the online journal.)

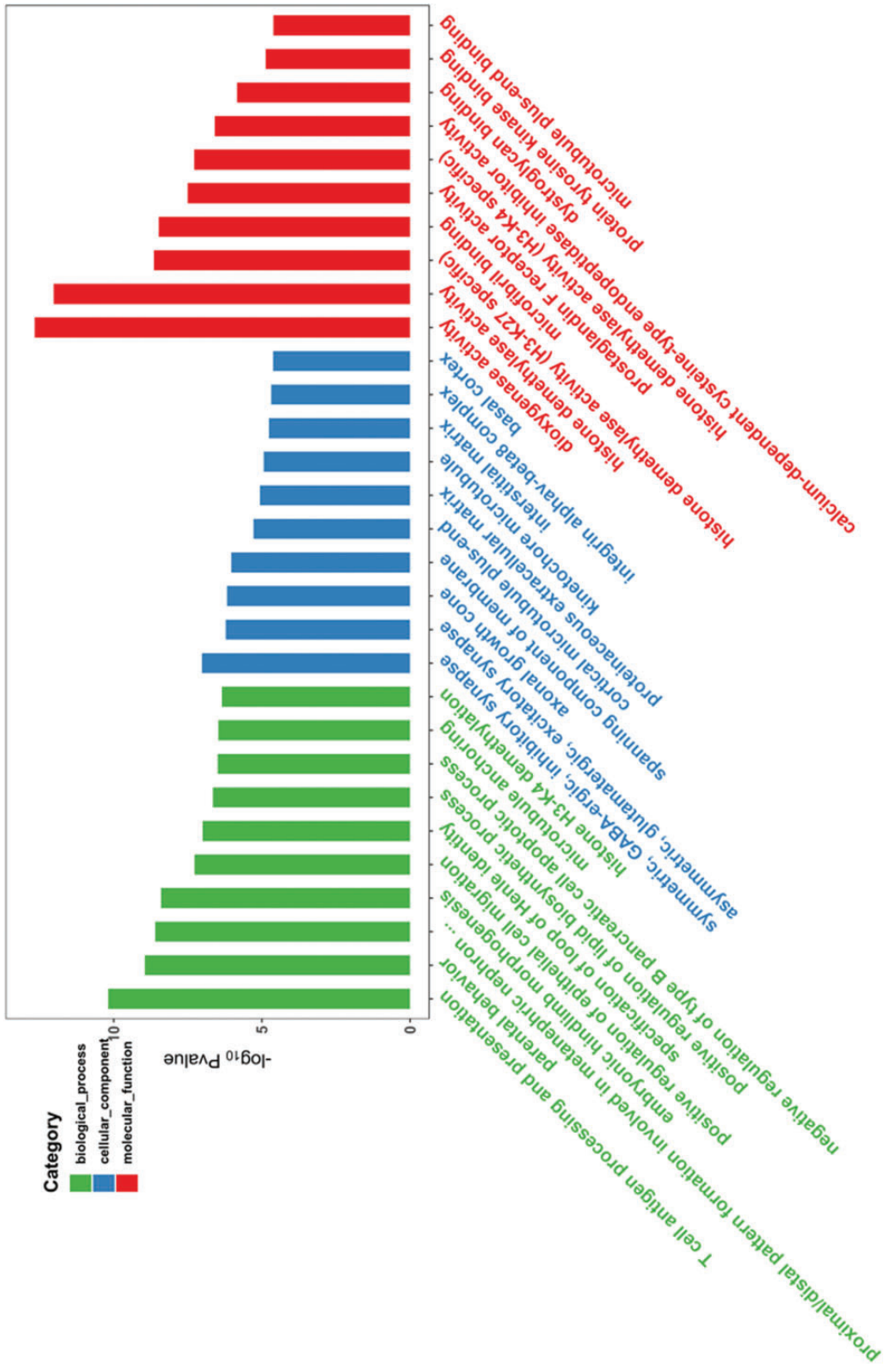

Figure 3. Gene Ontology (GO) function enrichment analysis of upregulated DET genes. Top 30 most significant GO terms of upregulated DET genes associated with biological processes (BP), cellular components (CC), and molecular functions (MF). (A color version of this figure is available in the online journal.)

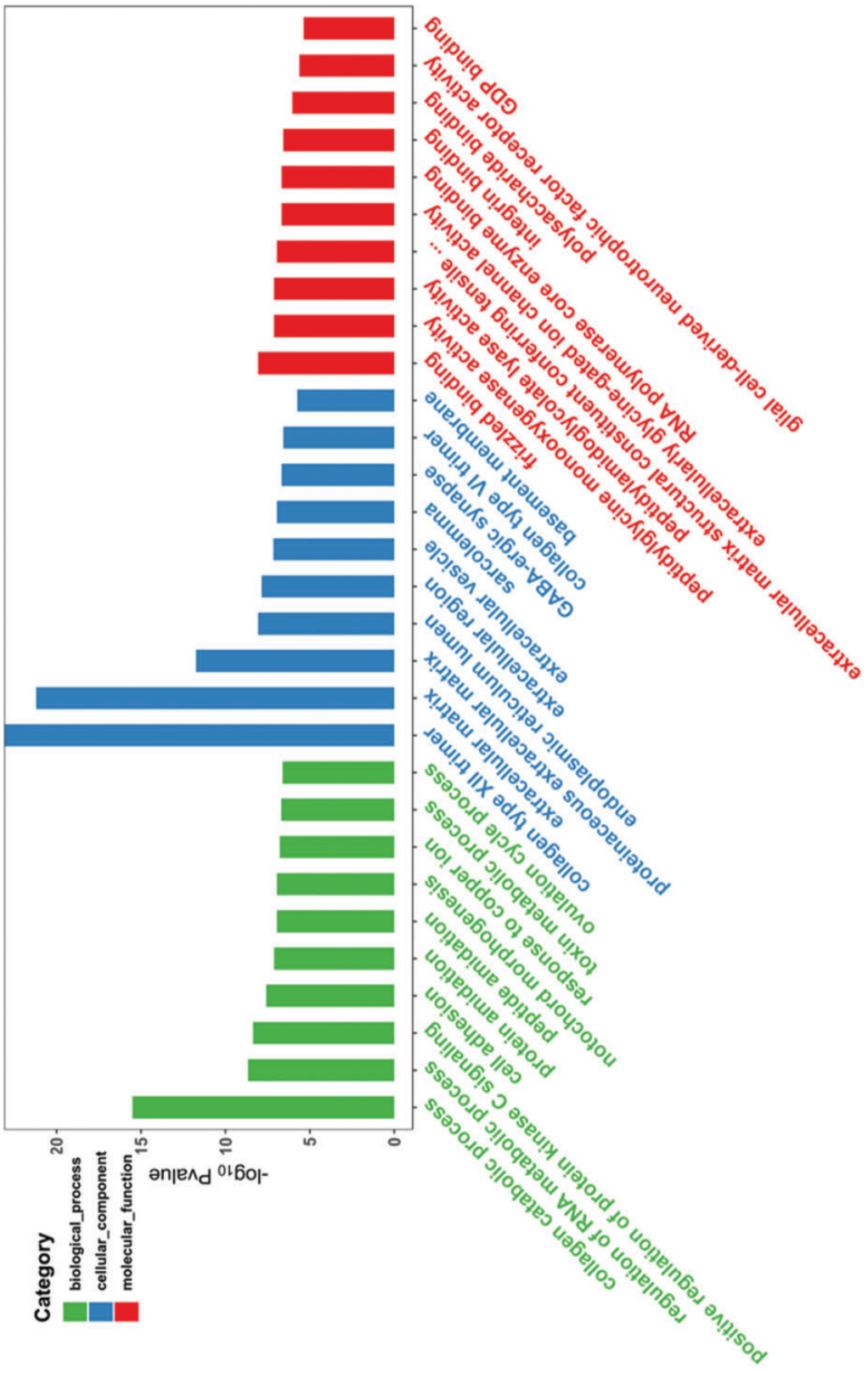

Figure 4. Gene Ontology (GO) function enrichment analysis of downregulated DET genes. Top 30 most significant GO terms of downregulated DET genes associated with biological processes (BP), cellular components (CC), and molecular functions (MF). (A color version of this figure is available in the online journal.)

Table 1. The top 30 GO terms of up- or down-regulated DET genes between TAO and control samples.

DET	ID	Term	Category	Gene
Upregulated	GO:0002457	T cell antigen processing and presentation	BP	KDM5D
	GO:0060746	Parental behavior	BP	ZFY
	GO:0072272	Proximal/distal pattern formation involved in metanephric nephron development	BP	IRX1; IRX2
	GO:0035116	Embryonic hindlimb morphogenesis	BP	PITX2; PITX1; ALX3; RSPO2; MED1; OSR2
	GO:0010634	Positive regulation of epithelial cell migration	BP	GLIPR2; CLASP2; CLASP1; DOCK1; DOCK5; CLASP2
	GO:0072086	Specification of loop of Henle identity	BP	IRX1; IRX2
	GO:0046889	Positive regulation of lipid biosynthetic process	BP	TCF7L2; SORBS1; CREB1; MLXIPL
	GO:2000675	Negative regulation of type b pancreatic cell apoptotic process	BP	CAST; TCF7L2
	GO:0034453	Microtubule anchoring	BP	PCM1; CLASP2; CLASP1
	GO:0034720	Histone h3-k4 demethylation	BP	KDM5D
	GO:0098983	Symmetric, gaba-ergic, inhibitory synapse	CC	NLGN4Y
	GO:0098985	Asymmetric, glutamatergic, excitatory synapse	CC	NLGN4Y
	GO:0044295	Axonal growth cone	CC	PARD3; BOC; GPM6A; FLRT3; CLASP2
	GO:0089717	Spanning component of membrane	CC	NLGN4Y
	GO:1903754	Cortical microtubule plus-end	CC	CLASP2
	GO:0005578	Proteinaceous extracellular matrix	CC	LTBP1; CPZ; LINGO2; ECM2; BGN; SPON1; LRRN1; WNT2B; PHOSPHO1; MATN2; FLRT3; ADAMTSL2; EPYC; PODN; COL24A1; COL19A1; FBLN5; FLRT2; GPLD1
	GO:0005828	Kinetochore microtubule	CC	CLASP2; CLASP1
	GO:0005614	Interstitial matrix	CC	VIT; ABI3BP; ECM2; KAZALD1; VWA1; ABI3BP; NAV2
	GO:0034686	Integrin alphav-beta8 complex	CC	ITGB8
	GO:0045180	Basal cortex	CC	CLASP2; CLASP1
	GO:0051213	Dioxygenase activity	MF	KDM5D; UTY; KDM6A; KDM3A
	GO:0032452	Histone demethylase activity	MF	KDM5D; UTY; KDM6A; KDM4B; KDM3A
	GO:0071558	Histone demethylase activity (H3-K27 specific)	MF	UTY; KDM6A
	GO:0050436	Microfibril binding	MF	LTBP1; ADAMTSL2
	GO:0004958	Prostaglandin F receptor activity	MF	PTGFR
	GO:0032453	Histone demethylase activity (H3-K4 specific)	MF	KDM5D
	GO:0010859	Calcium-dependent cysteine-type endopeptidase inhibitor activity	MF	CAST
	GO:0002162	Dystroglycan binding	MF	CLASP2; CLASP1
	GO:1990782	Protein tyrosine kinase binding	MF	CLASP2; HSP90AA1
	GO:0051010	Microtubule plus-end binding	MF	DST; CLASP2; CLASP1
Downregulated	GO:0030574	Collagen catabolic process	BP	COL5A1; CTSK; COL6A6; COL4A6; COL12A1; ADAMTS2; COL18A1; COL6A3; COL4A4; PHYKPL; MMP27
	GO:0051252	Regulation of RNA metabolic process	BP	NOVA1; RASA1
	GO:0090037	Positive regulation of protein kinase C signaling	BP	ADRA1A; VEGFA; WNT11
	GO:0007155	Cell adhesion	BP	COL5A1; ANOS1; LAMA2; CD44; COL6A6; CGREF1; EGFL6; ITGBL1; EDIL3; MAEA; NTM; COL4A6; COL12A1; FAP; THEMIS2; SPON2; SUSD5; TNXB; CD177; ADAM22; COL18A1; PCDHAC1; COL6A3; ERBIN; DST; ARHGAP5; MTSS1; EGFL7; PKN2; FER; EPHB4; PPFIBP1; NEO1; ADGRG1; MYH10; EMILIN2
	GO:0018032	Protein amidation	BP	PAM
	GO:0001519	Peptide amidation	BP	PAM

(continued)

Table 1. Continued.

DET	ID	Term	Category	Gene
	GO:0048570	Notochord morphogenesis	BP	WNT11; KDM6A
	GO:0046688	Response to copper ion	BP	PAM
	GO:0009404	Toxin metabolic process	BP	PAM
	GO:0022602	Ovulation cycle process	BP	PAM
	GO:0005595	Collagen type XII trimer	CC	COL12A1
	GO:0031012	Extracellular matrix	CC	COL5A1; FBN1; LAMA2; FBLN2; COL6A6; PRG4; SSC5D; EDIL3; HMCN2; MFAP5; JUP; CMA1; CPA3; CTSG; WNT2; COL12A1; ASPN; TNXB; COL18A1; COL6A3; ABI3BP; EGFL7; MMP27; EMILIN2
	GO:0005578	Proteinaceous extracellular matrix	CC	FBN1; ANOS1; FBLN2; COL6A6; PTPRZ1; OLFML2A; MFAP5; WNT2; WNT11; SPON2; ADAMTS2; ADAMTS7; ASPN; TNXB; WNT4; COL6A3; WNT16; ADAMTS16; MAMDC2; OLFML2A; IL1RL1; LINGO2; ADAMTSL1; EMILIN2; WNT5B; ADAMTS5
	GO:0005788	Endoplasmic reticulum lumen	CC	COL5A1; FBN1; CES1; ERAP1; SUMF1; SHISA5; COL4A6; COL12A1; ADAMTS7; COLGALT2; COL18A1; WNT4; COL6A3; COL4A4; ADAMTSL1; COL27A1; COLGALT1; EOGT; ARSJ; WNT5B; ADAMTS5
	GO:0005576	Extracellular region	CC	COL5A1; FBN1; ANOS1; CTSK; LAMA2; FBLN2; PNLIPRP3; FAM3C; ERAP1; FAM19A5; COL6A6; MFAP3; VASH2; NELL2; CGREF1; IL34; GHR; ENTPD5; CYB5D2; IST1; GUSB; MFAP5; DNASE1L1; ANGPT1; GCA; CAP1; NTM; JUP; FAM49B; IGSF1; CMA1; COL4A6; CPA3; CTSG; PSG5; TPSAB1; WNT2; LBP; COL12A1; WNT11; VEGFC; NELL1; TPSD1; ADAMTS2; APOL3; TNXB; SCUBE2; C14orf93; TPSB2; COL18A1; WNT4; FNDC1; RSPO3; ITIH5; COL6A3; WNT16; ANGPTL5; HSD17B13; FAM131A; ABI3BP; PRRG3; NTNG1; IMPDH2; FAM180A; VWCE; RGN; COL4A4; AOAH; EGFL7; COL27A1; CD163L1; TENM1; PDGFC; ARSJ; EPHB4; PLIN2; HABP4; EMILIN2; ENTPD6; WNT5B; HHIPL2; ADAMTS5; ATG7
	GO:1903561	Extracellular vesicle	CC	FBLN2; EDIL3; TUBB2A; COL12A1; COL6A3
	GO:0042383	Sarcolemma	CC	LAMA2; SGCE; AHNAK2; SLC8A1; ANK2; AHNAK; COL6A3; SGCZ; SLMAP; ANK3; KCNJ8
	GO:0098982	GABA-ergic synapse	CC	GLRB
	GO:0005589	Collagen type vi trimer	CC	COL6A3
	GO:0005604	Basement membrane	CC	COL5A1; FBN1; LAMA2; EGFL6; HMCN2; NTN4; COL18A1; CCDC80; ERBIN; DST; HMCN1
	GO:0005109	Frizzled binding	MF	WNT2; WNT11; WNT4; RSPO3; WNT16; WNT5B
	GO:0004504	Peptidylglycine monooxygenase activity	MF	PAM
	GO:0004598	Peptidylamidoglycolate lyase activity	MF	PAM
	GO:0030020	Extracellular matrix structural constituent conferring tensile strength	MF	COL12A1
	GO:0016933	Extracellularly glycine-gated ion channel activity	MF	GLRB
	GO:0043175	RNA polymerase core enzyme binding	MF	SCAF8
	GO:0005178	Integrin binding	MF	COL5A1; FBN1; TSPAN4; EGFL6; JAM3; EDIL3; FAP; TNXB; CD177; ADAM22; ITGB1BP1; ERBIN; DST; ADAMTS5
	GO:0030247	Polysaccharide binding	MF	PRG4
	GO:0016167	Glial cell-derived neurotrophic factor receptor activity	MF	GFRA1
	GO:0019003	GDP binding	MF	RAB28; RERG; RAP1B; RAB18; RRAGC; RAB27B; RALA; RAP2C

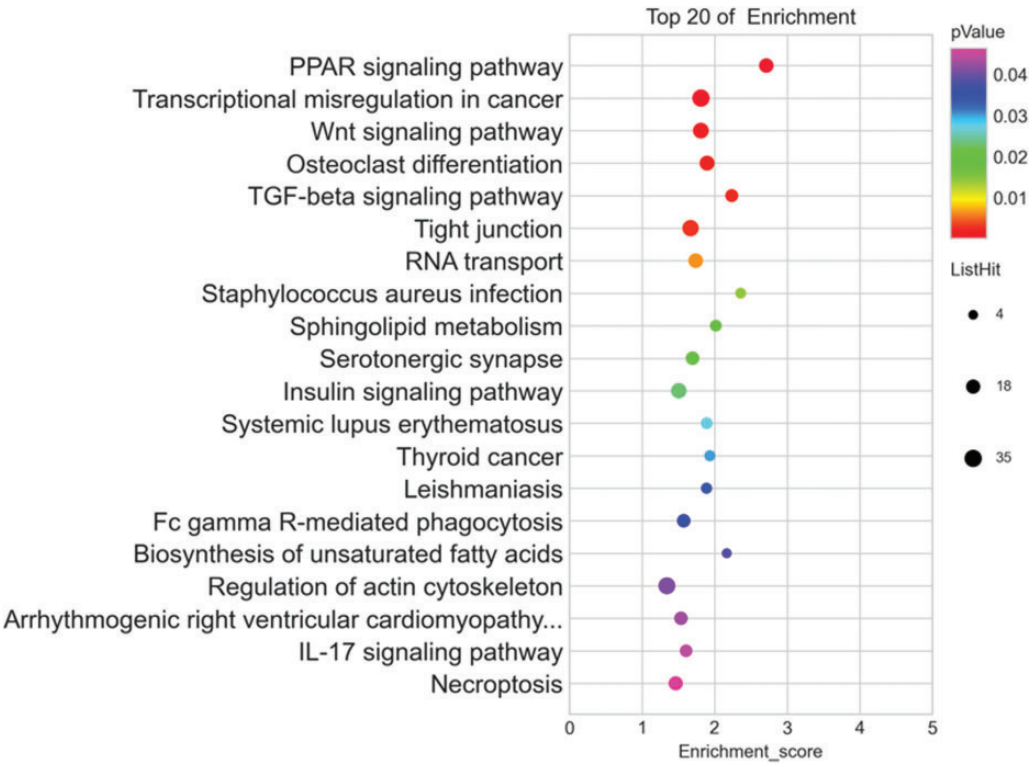

Figure 5. Kyoto Encyclopedia of Genes and Genomes (KEGG) pathway enrichment analysis of upregulated DET genes. Top 20 enriched KEGG pathways of upregulated DET genes. (A color version of this figure is available in the online journal.)

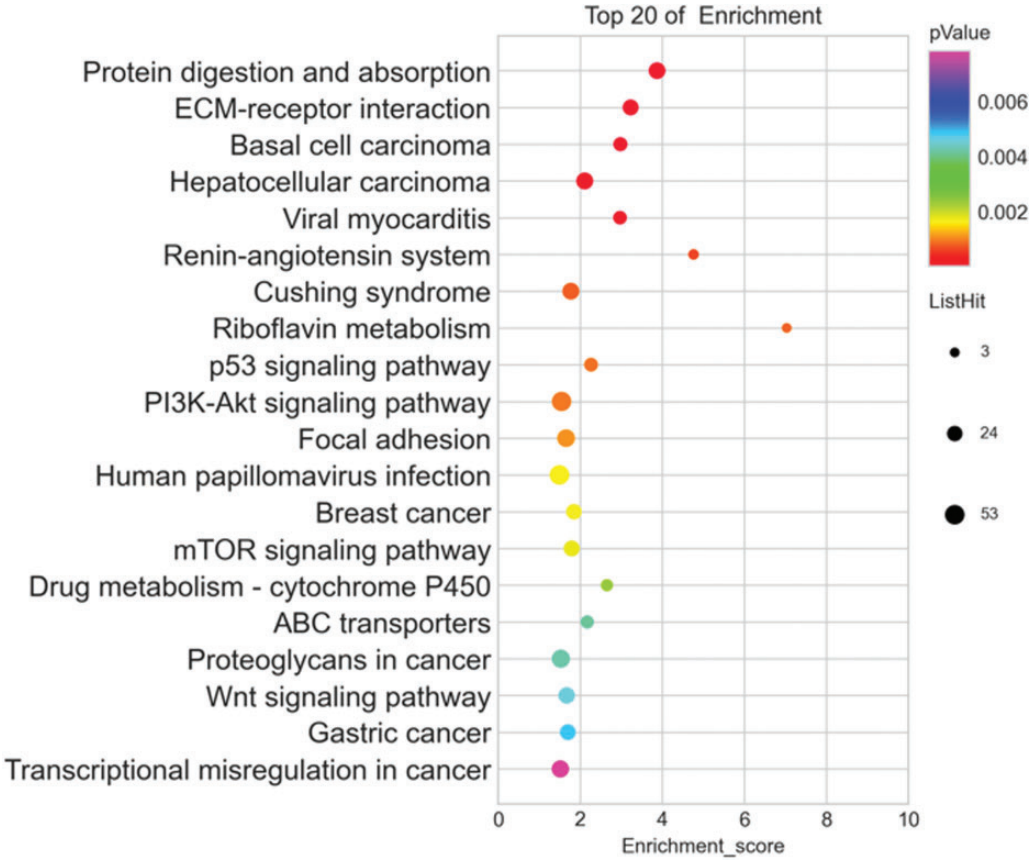

Figure 6. Kyoto Encyclopedia of Genes and Genomes (KEGG) pathway enrichment analysis of downregulated DET genes. Top 20 enriched KEGG pathways of downregulated DET genes. (A color version of this figure is available in the online journal.)

Table 2. The top 20 KEGG pathways of up- or down-regulated DET genes between TAO and control samples.

DET	ID	Term	Gene
Upregulated	hsa03320	PPAR signaling pathway	SLC27A6; ACOX3; PPARD; SORBS1; AQP7; PPARG; ACADL; FADS2; SCD; ACSL1; GK
	hsa05202	Transcriptional misregulation in cancer	EYA1; IL2RB; PLAT; UTY; KDM6A; ZEB1; PBX3; PTK2; PPARG; ATF1; FCGR1A; PBX1; NSD2; MDM2; RUNX1T1; ETV6; EWSR1; FUS; NCOR1
	hsa04310	Wnt signaling pathway	TCF7L2; PPARD; CCND3; CAMK2D; FZD2; SFRP2; WIF1; BAMBI; WNT2B; PRKACA; VANGL2; CTBP2; CAMK2G; PRICKLE2; MAPK10; PRICKLE1; TBL1Y
	hsa04380	Osteoclast differentiation	FOSB; FCGR3A; IL1R1; PPARG; CREB1; FCGR1A; TGFBR1; CYLD; STAT2; STAT1; MAPK10; MAPK14; LILRB3
	hsa04350	TGF-beta signaling pathway	PITX2; LTBP1; SMAD9; BMP5; BAMBI; TGFBR1; BMPR1B; RPS6KB1
	hsa04530	Tight junction	PARD3; CGNL1; RAPGEF2; TIAM1; CLDN11; MYH14; PRKACA; AFDN; MPDZ; DLG1; TJAP1; PATJ; MAPK10; PRKAG2; DLG2; ACTN4; NF2
	hsa03013	RNA transport	EIF4G3; NUP155; MAGOHB; NCBP1; EIF1AY; TGS1; RANBP2; UPF3A; SEH1L; RGPD1; SRRM1; RGPD5; FXR1
	hsa05150	*Staphylococcus aureus* infection	FCGR3A; C2; FPR1
	hsa00600	Sphingolipid metabolism	SMPD4; CERS1; CERS2; DEGS2; SMPD1; B4GALT6
	hsa04726	Serotonergic synapse	HTR2A; GNG4; PLA2G4B; CACNA1C; ALOX15; CYP4X1; GNG7; GNAO1; APP; PRKACA; ADCY5; MAOB
	hsa04910	Insulin signaling pathway	PHKA1; PYGL; SOCS2; SORBS1; PRKACA; MKNK1; PRKAR2B; ACACA; MAPK10; PRKAG2; RPS6KB1; SREBF1
	hsa05322	Systemic lupus erythematosus	FCGR3A; C2; HIST1H2BD; FCGR1A; ACTN4; TROVE2
	hsa05216	Thyroid cancer	TCF7L2; PPARG; TFG
	hsa05140	Leishmaniasis	FCGR3A; FCGR1A; STAT1; TLR2; MAPK14
	hsa04666	Fc gamma R-mediated phagocytosis	PLA2G4B; FCGR3A; GSN; PTPRC; PIP5K1B; FCGR1A; BIN1; RPS6KB1
	hsa01040	Biosynthesis of unsaturated fatty acids	ACOX3; FADS2; SCD; ELOVL7
	hsa04810	Regulation of actin cytoskeleton	GSN; FGFR1; SPATA13; PTK2; TIAM1; PIP5K1B; TMSB4Y; FGFR2; MYH14; ABI2; ITGA7; GNA12; DOCK1; CHRM3; ITGB8; ACTN4
	hsa05412	Arrhythmogenic right ventricular cardiomyopathy (ARVC)	CACNA1C; TCF7L2; CACNB4; SLC8A1; CACNA2D1; ITGA7; ITGB8
	hsa04657	IL-17 signaling pathway	FOSB; S100A8; LCN2; USP25; IL17RE; HSP90AA1; MAPK10; MAPK14
	hsa04217	Necroptosis	PLA2G4B; ALOX15; MLKL; PYGL; DNM1L; CAMK2D; CAMK2G; SMPD1; CYLD; CHMP2B; HSP90AA1; STAT2; STAT1; MAPK10
Downregulated	hsa04974	Protein digestion and absorption	COL5A1; COL6A6; SLC8A1; COL4A6; CPA3; DPP4; KCNN4; COL12A1; COL18A1; COL6A3; COL4A4; COL27A1; COL4A5
	hsa04512	ECM-receptor interaction	LAMA2; CD44; ITGA11; SDC1; COL6A6; COL4A6; THBS2; TNXB; COL6A3; COL4A4; COL4A5; SV2C; FN1
	hsa05217	Basal cell carcinoma	FZD6; TCF7L2; CDKN1A; APC; WNT2; WNT11; WNT4; WNT16; WNT5B
	hsa05225	Hepatocellular carcinoma	CDKN2A; NQO1; FZD6; TCF7L2; CDKN1A; NFE2L2; APC; WNT2; WNT11; SHC3; WNT4; WNT16; GSTM1; GAB1; PBRM1; MGST2; WNT5B; SMARCA4; PIK3CB
	hsa05416	Viral myocarditis	LAMA2; CD55; SGCA; EIF4G3; HLA-DQB1; BID; CASP9; SGCD; FYN
	hsa04614	Renin-angiotensin system	CMA1; CPA3; CTSG; AGTR1
	hsa04934	Cushing syndrome	CDKN2A; PDE11A; FZD6; TCF7L2; CDKN1A; RAP1B; APC; WNT2; WNT11; CDKN2B; AGTR1; RASD1; WNT4; WNT16; CAMK2G; CREB1; ARNT; WNT5B; PDE8A; PLCB4
	hsa00740	Riboflavin metabolism	ACP5; ENPP1
	hsa04115	p53 signaling pathway	CDKN2A; IGFBP3; RRM2B; CDKN1A; BID; SESN3; SHISA5; CASP9; MDM2; EI24; PERP
	hsa04151	PI3K-Akt signaling pathway	LAMA2; IL6; ITGA11; COL6A6; ANGPT2; CDKN1A; GHR; CASP9; VEGFA; ANGPT1; LPAR1; PTK2; PPP2R5C; PRKAA1; COL4A6; ERBB3; THBS2; VEGFD; VEGFC; SGK1; TNXB; COL6A3; BDNF; PPP2R1B; MDM2; COL4A4; CREB1; MAGI2; COL4A5; FOXO3; PKN2; FN1; PDGFC; PCK1; PIK3CB
	hsa04510	Focal adhesion	LAMA2; ITGA11; COL6A6; PARVB; RAP1B; VEGFA; MAPK8; PTK2; COL4A6; THBS2; VEGFD; VEGFC; SHC3; TNXB; COL6A3; ARHGAP5; COL4A4; BCAR1; COL4A5; FN1; MAPK10; PDGFC; FYN; PIK3CB

(continued)

Table 2. Continued.

DET	ID	Term	Gene
	hsa05165	*Human papillomavirus* infection	LAMA2; ITGA11; COL6A6; FZD6; TCF7L2; CDKN1A; VEGFA; PTK2; PPP2R5C; APC; COL4A6; THBS2; WNT2; WNT11; TNXB; WNT4; COL6A3; WNT16; PPP2R1B; TBK1; MDM2; COL4A4; CREB1; HDAC4; COL4A5; FN1; DLG1; UBE3A; WNT5B; PIK3CB
	hsa05224	Breast cancer	PGR; ESR1; FZD6; TCF7L2; CDKN1A; APC; WNT2; WNT11; SHC3; WNT4; WNT16; WNT5B; PIK3CB
	hsa04150	mTOR signaling pathway	MAPKAP1; PRR5; FZD6; SLC38A9; RRAGC; PRKAA1; WNT2; RPS6KA3; WNT11; SGK1; WNT4; WNT16; RNF152; TTI1; GRB10; ULK2; WNT5B; PIK3CB
	hsa00982	Drug metabolism - cytochrome P450	FMO3; FMO5; GSTM1; HPGDS; MGST2
	hsa02010	ABC transporters	ABCB5; ABCC10; ABCG1; ABCD4; ABCB11; ABCA6
	hsa05205	Proteoglycans in cancer	CD44; SDC1; ESR1; PLAU; FZD6; CDKN1A; VEGFA; MMP2; PTK2; ANK2; ERBB3; WNT2; WNT11; ANK1; WNT4; WNT16; GAB1; MDM2; ANK3; CAMK2G; FN1; WNT5B; PIK3CB
	hsa04310	Wnt signaling pathway	FZD6; TCF7L2; NFATC2; MAPK8; APC; WNT2; WNT11; DKK2; CTNNBIP1; WNT4; WNT16; PRICKLE2; CAMK2G; TBL1XR1; CTBP1; MAPK10; WNT5B; PLCB4
	hsa05226	Gastric cancer	FZD6; TCF7L2; CDKN1A; JUP; APC; WNT2; WNT11; CDKN2B; SHC3; WNT4; WNT16; GAB1; WNT5B; PIK3CB
	hsa05202	Transcriptional misregulation in cancer	IGFBP3; IL6; RUNX2; HIST2H3D; PLAU; EWSR1; RUNX1T1; CDKN1A; EYA1; PTK2; JUP; ETV6; MMP3; GRIA3; KDM6A; WNT16; NR4A3; MDM2; MLF1; ATF1; FUT8; NCOR1; MAF

pathway, which were involved in adipogenesis, inflammation, and immune response (Figure 5, Table 2). Enrichment pathways associated with downregulated mRNAs included protein digestion and absorption, ECM-receptor interaction, the PI3K/Akt signaling pathway, and the mTOR signaling pathway (Figure 6, Table 2). The results of KEGG analysis were consistent with the GO annotations.

Enrichment analysis of DAS genes

The function of DAS genes was also investigated using GO annotation and KEGG pathway analysis. As the most prevalent events in OACT of TAO, SE events mainly participated in the activation of Janus kinase activity (BP), protein localization to centrosome (BP), centrosome (CC), and actin binding (MF), which were associated with fibroblast migration, adipogenesis (cytoskeleton reorganization), and ECM remodeling (Figure 7). A3SS events were related to positive regulation of type I interferon production (BP), the centrosome cycle (BP), negative regulation of TOR signaling (BP), the microtubule cytoskeleton (CC), cytoskeletal adaptor activity (MF), and thyroid hormone receptor binding (MF) (Supplementary Figure 1(a)). A5SS events were related to cytoskeleton organization, negative regulation of type I interferon production (BP), the centrosome, the cytosol, the Z disc (CC), and the structural constituent of muscle (MF) (Supplementary Figure 2(a)). MXE events were related to the fatty acid metabolic process, smoothened signaling pathway, cilium assembly (BP), ECM (CC), metalloendopeptidase activity, and actin binding (MF) (Supplementary Figure 3(a)).

The top 20 KEGG enrichment pathways of DAS genes are shown in Figure 5. SE events of DAS genes were involved in fatty acid biosynthesis, the PPAR signaling pathway, glycerophospholipid metabolism, and adherens junction, which were related to adipogenesis in TAO (Figure 8). A3SS events were involved in fatty acid degradation, glycerophospholipid metabolism, the toll-like receptor signaling pathway, thyroid hormone synthesis, and the PPAR signaling pathway (Supplementary Figure 1(b)). A5SS events were involved in the regulation of lipolysis in adipocytes, the adipocytokine signaling pathway, and Th1/Th2 cell differentiation (Supplementary Figure 2 (b)). MXE events were involved in the regulation of lipolysis in adipocytes, the PPAR signaling pathway, the JAK/STAT signaling pathway, and cytokine–cytokine receptor interaction (Supplementary Figure 3(b)).

In summary, the enriched GO terms and KEGG pathways in DAS genes were largely associated with adipogenesis and ECM remodeling, which is consistent with the results of the DET gene enrichment analysis.

Validation of the expression of DET genes

In accordance with the differential expression analysis, the samples of TAO patients exhibited differential splicing transcript expression of *VCAN*, *SORBS1*, *SEPT2*, and *COL12A1*. To validate the RNA sequencing results, we detected the expression levels of transcript variant 1

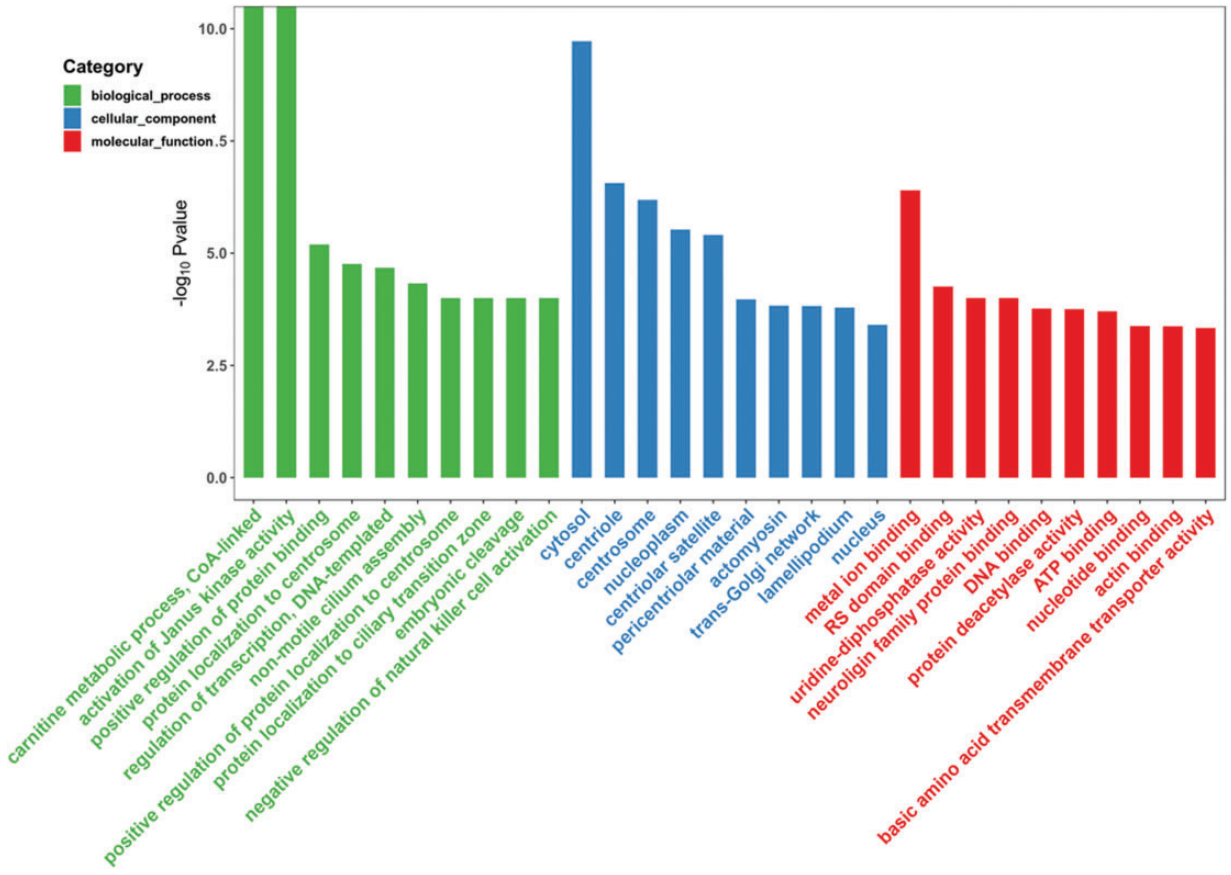

Figure 7. Gene Ontology (GO) function enrichment analysis of DAS genes edited by SE events. Top 30 most significant GO terms in BP, CC, and MF of DAS genes edited by SE events. (A color version of this figure is available in the online journal.)

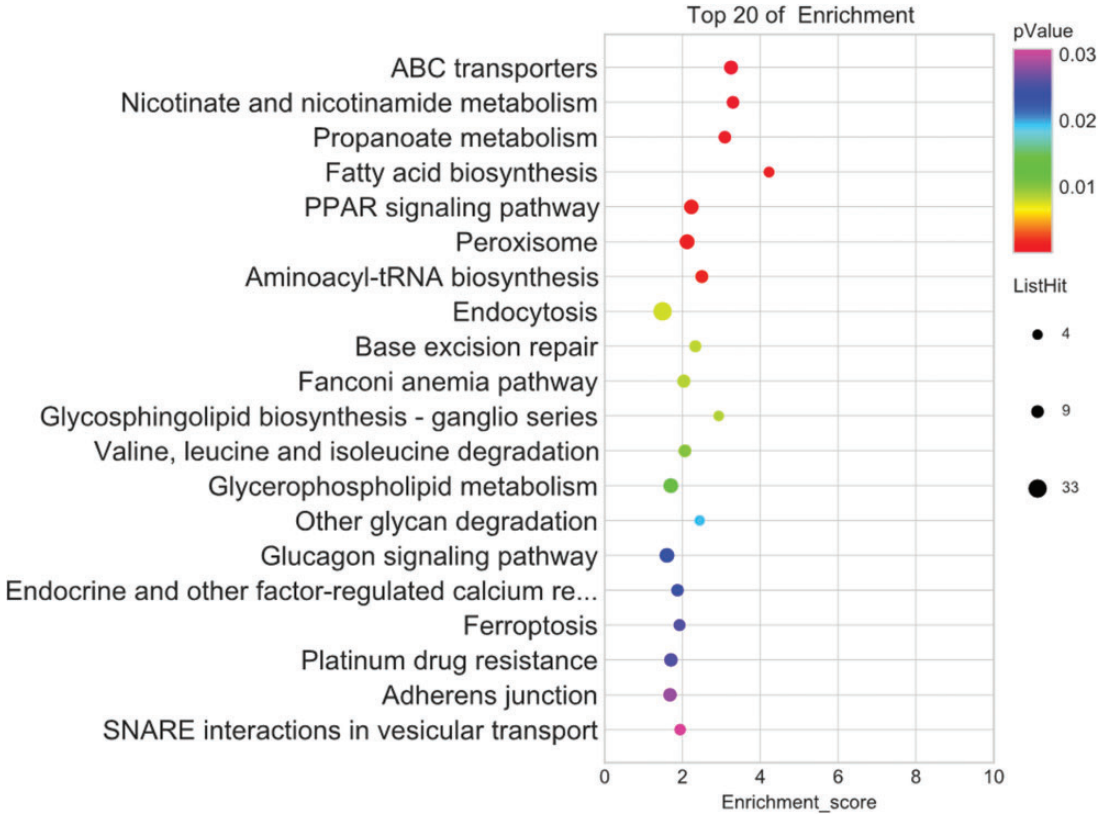

Figure 8. Kyoto Encyclopedia of Genes and Genomes (KEGG) pathway enrichment analysis of DAS genes edited by SE events. Top 20 enriched KEGG pathways of DAS genes edited by SE events. (A color version of this figure is available in the online journal.)

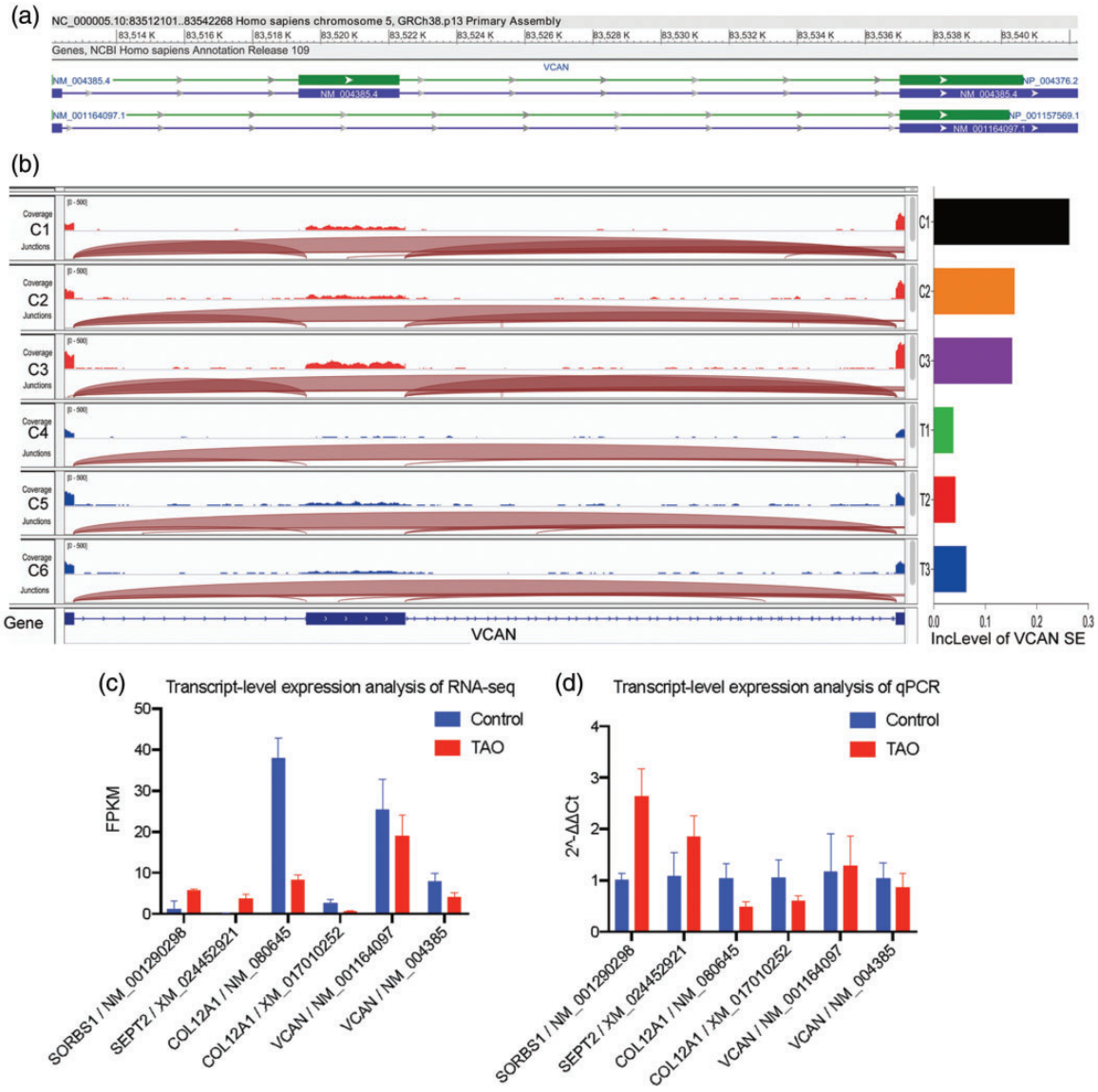

Figure 9. Validation of the expression of DET genes in TAO and control samples. (a) Sequences and exon distribution in transcripts NM_004385.4 and NM_001164097.1 of the VCAN gene. (b) Level of exon inclusion reads, which represents the reads across the junction between exons, of VCAN in TAO and control samples. (c) Expression levels of six transcripts from four genes (SORBS1, SEPT2, COL12A1, and VCAN) based on the RNA sequencing data. (d) Expression levels of six transcripts from four genes based on the qRT-PCR results. (A color version of this figure is available in the online journal.)

(NM_004385.4) and transcript variant 3 (NM_001164097.1) of *VCAN*, transcript variant 12 (NM_001290298.1) of *SORBS1*, transcript variant X2 (XM_024452921.1) of *SEPT2*, and transcript variant short (NM_080645.2) and transcript variant X2 (XM_017010252.2) of *COL12A1*.

Transcript NM_001164097.1 of *VCAN* lacked an exon in the coding region compared with transcript NM_004385.4 (Figure 9(a)). The RNA sequencing analysis revealed that the levels of exon inclusion reads and NM_004385.4 of *VCAN* were lower in TAO patients (Figure 9(b) and (c)), indicating that the occurrence of SE events in *VCAN* was more frequent in TAO patients' samples than in those of controls. Moreover, transcript NM_001290298.1 of *SORBS1* and transcript XM_024452921.1 of *SEPT2* were upregulated, whereas transcripts NM_080645.2 and XM_017010252.2 of *COL12A1* were downregulated (Figure 9(c)). The qRT-PCR results confirmed that the expression levels of NM_001290298.1 of *SORBS1* and XM_024452921.1 of *SEPT2* were elevated, whereas the levels of NM_080645.2 and XM_017010252.2 of *COL12A1* and NM_004385.4 of *VCAN* were reduced (Figure 9(d)). Thus, the qRT-PCR results were consistent with the RNA sequencing results.

Discussion

TAO is characterized by the remodeling and expansion of orbital tissue. Dysregulated metabolism of the ECM and increased orbital adipose/connective tissue are considered the two major elements associated with the pathogenesis of TAO. However, the underlying mechanism is not yet fully understood. In this study, we used RNA sequencing to analyze the DET and DAS genes in OACT of TAO patients in order to investigate the genetic regulation of TAO. Among 113,095 identified genes from RNA sequencing data, 3096

DETs were predicted, of which 1460 were upregulated and 1636 were downregulated. Moreover, 4278 DAS genes were compared between TAO patients and control subjects. Among five main AS events, SE events were the most prevalent, accounting for 66.48%, while RI events were the rarest, accounting for 2.59%. The results indicated the prevalence and importance of the mechanism of AS in the regulation of TAO. Moreover, SE events may play a critical role in the pathological changes of adipose/connective tissue.

The enriched GO terms and KEGG pathways provided more insights into the role of DET and DAS genes in TAO. Based on the results, we found that numerous DETs were associated with the autoimmune response, ECM remodeling, and adipogenesis in adipose/connective tissue. T cell infiltration is a major trigger of pathogenesis in the orbit.[28] In terms of GO analysis, DETs associated with the BP of T cell antigen presentation (GO:0002457) may influence the function of immune cells. The pathway analysis revealed the relationship between DETs and cytokine signaling pathways, including TGF-β (hsa04380) and IL-17 (hsa04657). Aberrant cytokine signaling plays a critical role in the pathogenesis of TAO. Growing evidence shows that the cytokine profile is derived not only from monocytes/macrophages and lymphocytes but also from thyrocytes, OFs, and even adipocytes, participating in inflammation and fibroblast activation in adipose/connective tissue.[28] IL-17A can significantly promote the proinflammatory and profibrotic functions of OFs.[29] Moreover, in the presence of proinflammatory signaling, TGF-β promotes the differentiation of naïve CD4+ T cells into Th17 cells, which mainly produces IL-17.[30] Hence, TGF-β and IL-17 cooperate in promoting TAO.

DETs were associated with the CC of the ECM (GO:0031012), the BPs of the collagen catabolic process (GO:0030574) and cell adhesion (GO:0007155), and the MF of integrin binding (GO:0005178). The ECM-receptor interaction pathway (hsa04512), associated with downregulated DETs, was also screened out. Profound ECM remodeling mediated by activated fibroblasts is a major process in TAO.[5] The accumulation of ECM components, such as collagen, is a hallmark of ECM remodeling and provides multiple potential autoantigens to exacerbate an aberrant autoimmune response.[31] Previous studies have demonstrated that integrin-dependent pathways mediate the recruitment of activated T lymphocytes in the retro-orbital space.[32] Impaired interaction between T cells and the ECM also stimulates this process.[33]

The GO terms related to the microtubule cytoskeleton function (GO:0034453, GO:0005828, and GO:0051010) predicted that the related transcripts modulated the adipogenesis of OFs.[34] The KEGG analysis revealed that the DETs were associated with pathways such as the PPAR signaling pathway (hsa03320), the insulin signaling pathway (hsa04910), the PI3K/Akt signaling pathway (hsa04151), and the mTOR signaling pathway (hsa04150), which are also closely related to adipogenesis.[7,35] Growing evidence shows that the increased volume of the orbital space is largely due to the adipogenesis process. OFs cultured from TAO mouse models with high TSHR and IGF-1R levels exhibited increased adipogenesis, indicating its important role in TAO.[36] PPARγ is the most important transcriptional modulator in adipogenesis.[37] It has been found that the level of PPARγ is positively correlated with adipogenesis and the level of TSHR in adipose/connective tissues of TAO patients.[38] Another member of the PPAR family, PPARα, also participates in modulating the secretion of CXCL8 and CXCL10 of OFs and preadipocytes, which regulate the inflammatory response.[39] IGF-1 and IGF-1R also play major roles in TAO. IGF-1R is an autoantigen on the cell surface that can form a physical and functional signaling complex with TSHR on fibrocytes, contributing to the transduction of downstream signaling.[40] A randomized placebo-controlled trial investigated human IGF-1R-inhibiting monoclonal antibody teprotumumab as a potential therapeutic strategy to attenuate pathogenesis, producing good outcomes compared with the placebo.[41] Consequently, the related DETs are also potential regulators of the pathogenesis of TAO.

Our DAS analysis showed that differential AS events were also significantly related to the above processes, especially adipogenesis. AS leads to the generation of differential splicing transcripts from one gene, which can be translated into differential functional isoforms. In the DAS analysis, we found that the enriched GO terms associated with AS events were related to centrosome, actin, and microtubule functions. Other GO terms included the BF of positive regulation of type I interferon production, the MF of thyroid hormone receptor binding, the CC of the ECM, and the MF of metalloendopeptidase activity, which were related to cytokine function and ECM remodeling. The KEGG pathway analysis revealed the most enriched pathways, including fatty acid biosynthesis, the PPAR signaling pathway, glycerophospholipid metabolism, and adherens junction. Microtubules and actin filaments are the two main cytoskeleton networks supporting the intracellular architecture and the centrosome, which are considered the organizing centers of both.[42] Cytoskeleton changes interacting with the ECM and influencing the shape and function of cells are observed during adipogenesis.[43,44] However, their role in TAO has not yet been elucidated. On the other hand, several pathways have been integratedly analyzed. Fatty acid biosynthesis and glycerophospholipid metabolism are critical parts of adipogenesis, with close interactions with the PPAR family.[45]

Our analysis showed a remarkable overlap between the functions of DET and DAS genes. Among them, *SORBS1* encodes Cbl-associated protein (CAP), which plays a role in signaling transduction and cytoskeleton rearrangement. CAP is enriched in insulin-sensitive tissues and participates in the insulin signaling pathway and in adipocyte differentiation.[46] A PPAR response element in its promoter has been identified in the sequence of *SORBS1*, which can regulate the level of CAP.[47] Our analysis revealed one transcript of *SORBS1* upregulated in TAO patients, suggesting its potential regulatory function in adipogenesis. The septin family is involved in cytoskeleton reorganization, cytokinesis, and membrane dynamics.[48] Little is known about the exact function of septin-2, encoded by the *SEPT2* gene, in TAO. However, PPARγ can regulate the expression and function of *SEPT2* in hepatoma cells,[49] suggesting the potential role of *SEPT2* in cytoskeleton regulation and

PPAR-mediated signaling. Our results showed opposite expression patterns in two transcripts of *SEPT2*. The importance of this difference remains to be studied.

Collagen XII is a critical component of the ECM, helping to maintain its structure and function. AS of *COL12A1* results in a large isoform collagen (XIIA; 320 kD) and a short isoform collagen (XIIB; 220 kD).[50] Collagen XIIA has an NC3 domain carrying glycosaminoglycan chains, whereas collagen XIIB does not. We only discovered low levels of the short splicing transcript, which is involved in the collagen catabolic process according to the GO terms. *VCAN* encodes versican, an ECM proteoglycan associated with glycosaminoglycan metabolism, which potentially influences TAO. The protein domains encoded by exons 7 and 8 can attach to glycosaminoglycan residues,[51] while AS produces different transcripts either containing these exons or not. According to our analysis, SE events were more prevalent in *VCAN* genes of TAO patients, indicating high expression of transcripts without exon 7. This also suggests the modulatory role of AS in TAO.

Taken together, the integrated analysis of DET and DAS genes demonstrated that multiple pathways modulating the development of TAO are regulated by the mechanism of AS, resulting in the differential expression of diverse functional transcripts. In particular, the upregulation of components and pathways associated with adipogenesis in our analysis is notable. However, previous studies have reported contradictory results regarding the stimulation of adipogenesis-inhibiting pathways. A study showed that the TGF-β and IL-17 signaling pathways promote fibrosis of Thy+ orbital fibroblasts but inhibit the adipogenesis of Thy−OFs.[52] Moreover, PGF-2α suppresses the function of PPARγ and activates the MEK/ERK cascade, inhibiting the early phase of adipogenesis through prostaglandin F receptor.[53] In our study, PGF receptor activity and the TGF-β/IL-17 signaling pathway were related to upregulated DETs. It is assumed that they exert a potentially protective effect against adipogenesis, which is indicative of the complex modulatory network of adipogenesis and inflammation. Previous research has revealed increased inflammation and adipogenesis in active TAO, which can be attenuated in inactive TAO.[54] Thus, some pathways associated with the inhibition of adipogenesis and the activation of fibrosis may be triggered in response to a change in TAO activity. In our study, the TAO patient tissue samples were in the inactive phase. Hence, it is possible that some adipogenesis-inhibiting signaling pathways were significantly activated. More attention should be paid to AS events to explore new biomarkers and therapeutic targets for TAO and to study changes in AS events during the different phases of TAO.

Conclusions

In this study, we conducted an analysis of DET and DAS genes of adipose/connective tissues of TAO patients, predicting 3096 DETs and 4278 DAS genes. Using rMATS, we found that SE is the most prevalent of all AS events. GO and KEGG analysis showed that the most enriched functions are related to the immune response, ECM remodeling, and adipogenesis. Our results suggest a potentially important role of AS in the pathogenesis of TAO. AS of candidate genes may provide insights into the underlying mechanisms and new therapeutic targets for TAO in the near future.

AUTHORS' CONTRIBUTIONS

Lianqun Wu conceived and designed the experiments. Lianqun Wu and Yu Liang participated in the paper writing. Xiying Wang and Chao Jiang performed the experiments. Nan Song and Xinxin Chen collected the samples. Bing Qin, Xiantao Sun, and Guohua Liu analyzed the data. Chen Zhao supervised the progress and revised the manuscript. All authors read and approved the final manuscript.

ACKNOWLEDGEMENTS

The authors thank Professor Ruili Wei (Department of Ophthalmology, Changzheng Hospital, Second Military Medical University) for providing orbital adipose/connective tissue samples of TAO patients. For bioinformatics analysis, the authors appreciated the assistance of Dr. Yao Cheng (OE Biotech, Inc., Shanghai, China, http://www.oebiotech.com/).

DECLARATION OF CONFLICTING INTERESTS

The authors declared no potential conflicts of interest with respect to the research, authorship, and/or publication of this article.

ETHICAL APPROVAL

The study was approved in China by the Ethics Committee of Changzheng Hospital, Second Military Medical University (2018SL039A). All patients got written informed consent, and the research protocol followed the principle of the Declaration of Helsinki.

FUNDING

This study was supported by Shanghai Natural Science Foundation (20ZR1409800 to L.Q.W), National Natural Science Foundation of China (81600765 to L.Q.W., 81670864 and 81730025 to C.Z.), Excellent Academic Leaders of Shanghai (18XD1401000 to C.Z.), Shanghai Municipal Health and Family Planning Commission (201640120 to L.Q.W.).

ORCID iD

Chen Zhao https://orcid.org/0000-0003-1373-7637

SUPPLEMENTAL MATERIAL

Supplemental material for this article is available online.

REFERENCES

1. Bahn RS. Graves' ophthalmopathy. *N Engl J Med* 2010;**362**:726–38
2. McGregor AM. Has the target autoantigen for Graves' ophthalmopathy been found? *Lancet* 1998;**352**:595–6
3. Wall JR, Lahooti H. Pathogenesis of thyroid eye disease – does autoimmunity against the TSH receptor explain all cases? *Endokrynol Pol* 2010;**61**:222–7

4. Feldon SE, Park DJ, O'Loughlin CW, Nguyen VT, Landskroner-Eiger S, Chang D, Thatcher TH, Phipps RP. Autologous T-lymphocytes stimulate proliferation of orbital fibroblasts derived from patients with Graves' ophthalmopathy. *Invest Ophthalmol Vis Sci* 2005;**46**:3913–21
5. Eckstein AK, Johnson KT, Thanos M, Esser J, Ludgate M. Current insights into the pathogenesis of Graves' orbitopathy. *Horm Metab Res* 2009;**41**:456–64
6. Valyasevi RW, Harteneck DA, Dutton CM, Bahn RS. Stimulation of adipogenesis, peroxisome proliferator-activated receptor-gamma (PPARgamma), and thyrotropin receptor by PPARgamma agonist in human orbital preadipocyte fibroblasts. *J Clin Endocrinol Metab* 2002;**87**:2352–8
7. Zhao P, Deng Y, Gu P, Wang Y, Zhou H, Hu Y, Chen P, Fan X. Insulin-like growth factor 1 promotes the proliferation and adipogenesis of orbital adipose-derived stromal cells in thyroid-associated ophthalmopathy. *Exp Eye Res* 2013;**107**:65–73
8. Bahn RS. Thyrotropin receptor expression in orbital adipose/connective tissues from patients with thyroid-associated ophthalmopathy. *Thyroid* 2002;**12**:193–5
9. Yang HW, Wang YX, Bao J, Wang SH, Lei P, Sun ZL. Correlation of HLA-DQ and TNF-α gene polymorphisms with ocular myasthenia gravis combined with thyroid-associated ophthalmopathy. *Biosci Rep* 2017;**37**:BSR20160440
10. Zhao P, Yin H, Tao C, Chen P, Song Y, Yang W, Liu L. Latent pathways identification by microarray expression profiles in thyroid-associated ophthalmopathy patients. *Endocr Pathol* 2015;**26**:200–10
11. Tong BD, Xiao MY, Zeng JX, Xiong W. MiRNA-21 promotes fibrosis in orbital fibroblasts from thyroid-associated ophthalmopathy. *Mol Vis* 2015;**21**:324–34
12. Wu L, Zhou R, Diao J, Chen X, Huang J, Xu K, Ling L, Xia W, Liang Y, Liu G, Sun X, Qin B, Zhao C. Differentially expressed circular RNAs in orbital adipose/connective tissue from patients with thyroid-associated ophthalmopathy. *Exp Eye Res* 2020;**196**:108036
13. Wang Y, Liu J, Huang BO, Xu YM, Li J, Huang LF, Lin J, Zhang J, Min QH, Yang WM, Wang XZ. Mechanism of alternative splicing and its regulation. *Biomed Rep* 2015;**3**:152–8
14. Lin JC. Impacts of alternative splicing events on the differentiation of adipocytes. *Int J Mol Sci* 2015;**16**:22169–89
15. Liu H, Lorenzini PA, Zhang F, Xu S, Wong MSM, Zheng J, Roca X. Alternative splicing analysis in human monocytes and macrophages reveals MBNL1 as major regulator. *Nucleic Acids Res* 2018;**46**:6069–86
16. Pujol-Lereis LM, Liebisch G, Schick T, Lin Y, Grassmann F, Uchida K, Zipfel PF, Fauser S, Skerka C, Weber BHF. Evaluation of serum sphingolipids and the influence of genetic risk factors in age-related macular degeneration. *PLoS One* 2018;**13**:e0200739
17. Cardamone G, Paraboschi EM, Rimoldi V, Duga S, Soldà G, Asselta R. The characterization of GSDMB splicing and backsplicing profiles identifies novel isoforms and a circular RNA that are dysregulated in multiple sclerosis. *Int J Mol Sci* 2017;**18**:576
18. Farina AR, Cappabianca L, Sebastiano M, Zelli V, Guadagni S, Mackay AR. Hypoxia-induced alternative splicing: the 11th hallmark of cancer. *J Exp Clin Cancer Res* 2020;**39**:110
19. Bartley GB, Gorman CA. Diagnostic criteria for Graves' ophthalmopathy. *Am J Ophthalmol* 1995;**119**:792–5
20. Mourits MP, Prummel MF, Wiersinga WM, Koornneef L. Clinical activity score as a guide in the management of patients with Graves' ophthalmopathy. *Clin Endocrinol* 1997;**47**:9–14
21. Bolger AM, Lohse M, Usadel B. Trimmomatic: a flexible trimmer for illumina sequence data. *Bioinformatics* 2014;**30**:2114–20
22. Kim D, Langmead B, Salzberg SL. HISAT: a fast spliced aligner with low memory requirements. *Nat Methods* 2015;**12**:357–60
23. Anders S, Pyl PT, Huber W. HTSeq – a python framework to work with high-throughput sequencing data. *Bioinformatics* 2015;**31**:166–9
24. Roberts A, Pimentel H, Trapnell C, Pachter L. Identification of novel transcripts in annotated genomes using RNA-Seq. *Bioinformatics* 2011;**27**:2325–9
25. Anders S, Huber W. Differential expression analysis for sequence count data. *Genome Biol* 2010;**11**:R106
26. Shen S, Park JW, Lu ZX, Lin L, Henry MD, Wu YN, Zhou Q, Xing Y. rMATS: robust and flexible detection of differential alternative splicing from replicate RNA-Seq data. *Proc Natl Acad Sci U S A* 2014;**111**:E5593–601
27. Wang L, Cao C, Ma Q, Zeng Q, Wang H, Cheng Z, Zhu G, Qi J, Ma H, Nian H, Wang Y. RNA-seq analyses of multiple meristems of soybean: novel and alternative transcripts, evolutionary and functional implications. *BMC Plant Biol* 2014;**14**:169
28. Gianoukakis AG, Khadavi N, Smith TJ. Cytokines, Graves' disease, and thyroid-associated ophthalmopathy. *Thyroid* 2008;**18**:953–8
29. Fang S, Huang Y, Wang S, Zhang Y, Luo X, Liu L, Zhong S, Liu X, Li D, Liang R, Miranda P, Gu P, Zhou H, Fan X, Li B. IL-17A exacerbates fibrosis by promoting the proinflammatory and profibrotic function of orbital fibroblasts in TAO. *J Clin Endocrinol Metab* 2016;**101**:2955–65
30. Lee GR. The balance of Th17 versus treg cells in autoimmunity. *Int J Mol Sci* 2018;**19**:730
31. Bednarczuk T, Stolarski C, Pawlik E, Slon M, Rowinski M, Kubota S, Hiromatsu Y, Bartoszewicz Z, Wall JR, Nauman J. Autoantibodies reactive with extracellular matrix proteins in patients with thyroid-associated ophthalmopathy. *Thyroid* 1999;**9**:289–95
32. Heufelder AE, Scriba PC. Characterization of adhesion receptors on cultured microvascular endothelial cells derived from the retroorbital connective tissue of patients with Grave's ophthalmopathy. *Eur J Endocrinol* 1996;**134**:51–60
33. Bednarczuk T, Kiljanski J, Mrowiec T, Slon M, Ing E, Stolarski C, Kennerdell JS, Gorski A, Nauman J, Wall JR. T cell interactions with extracellular matrix proteins in patients with thyroid-associated ophthalmopathy. *Autoimmunity* 1998;**27**:221–30
34. Padilla-Benavides T, Velez-delValle C, Marsch-Moreno M, Castro-Muñozledo F, Kuri-Harcuch W. Lipogenic enzymes complexes and cytoplasmic lipid droplet formation during adipogenesis. *J Cell Biochem* 2016;**117**:2315–26
35. Cai H, Dong LQ, Liu F. Recent advances in adipose mTOR signaling and function: therapeutic prospects. *Trends Pharmacol Sci* 2016;**37**:303–17
36. Görtz GE, Moshkelgosha S, Jesenek C, Edelmann B, Horstmann M, Banga JP, Eckstein A, Berchner-Pfannschmidt U. Pathogenic phenotype of adipogenesis and hyaluronan in orbital fibroblasts from female Graves' orbitopathy mouse model. *Endocrinology* 2016;**157**:3771–8
37. Mota de Sá P, Richard AJ, Hang H, Stephens JM. Transcriptional regulation of adipogenesis. *Compr Physiol* 2017;**7**:635–74
38. Kumar S, Coenen MJ, Scherer PE, Bahn RS. Evidence for enhanced adipogenesis in the orbits of patients with Graves' ophthalmopathy. *J Clin Endocrinol Metab* 2004;**89**:930–5
39. Ferrari SM, Ragusa F, Paparo SR, Nasini F, Nardi M, Franceschini SS, Fallahi P, Antonelli A. Differential modulation of CXCL8 versus CXCL10, by cytokines, PPAR-gamma, or PPAR-alpha agonists, in primary cells from Graves' disease and ophthalmopathy. *Autoimmun Rev* 2019;**18**:673–8
40. Smith TJ, Janssen J. Insulin-like growth factor-I receptor and thyroid-associated ophthalmopathy. *Endocr Rev* 2019;**40**:236–67
41. Smith TJ, Kahaly GJ, Ezra DG, Fleming JC, Dailey RA, Tang RA, Harris GJ, Antonelli A, Salvi M, Goldberg RA, Gigantelli JW, Couch SM, Shriver EM, Hayek BR, Hink EM, Woodward RM, Gabriel K, Magni G, Douglas RS. Teprotumumab for thyroid-associated ophthalmopathy. *N Engl J Med* 2017;**376**:1748–61
42. Farina F, Gaillard J, Guérin C, Couté Y, Sillibourne J, Blanchoin L, Théry M. The centrosome is an actin-organizing Centre. *Nat Cell Biol* 2016;**18**:65–75
43. Mor-Yossef Moldovan L, Lustig M, Naftaly A, Mardamshina M, Geiger T, Gefen A, Benayahu D. Cell shape alteration during adipogenesis is associated with coordinated matrix cues. *J Cell Physiol* 2019;**234**:3850–63
44. Trivanović D, Drvenica I, Kukolj T, Obradović H, Okić Djordjević I, Mojsilović S, Krstić J, Bugarski B, Jauković A, Bugarski D. Adipoinductive effect of extracellular matrix involves cytoskeleton changes and SIRT1 activity in adipose tissue stem/stromal cells. *Artif Cells Nanomed Biotechnol* 2018;**46**:S370–82

45. Barquissau V, Ghandour RA, Ailhaud G, Klingenspor M, Langin D, Amri EZ, Pisani DF. Control of adipogenesis by oxylipins, GPCRs and PPARs. *Biochimie* 2017;**136**:3–11
46. Zhang M, Kimura A, Saltiel AR. Cloning and characterization of cbl-associated protein splicing isoforms. *Mol Med* 2003;**9**:18–25
47. Baumann CA, Chokshi N, Saltiel AR, Ribon V. Cloning and characterization of a functional peroxisome proliferator activator receptor-gamma-responsive element in the promoter of the CAP gene. *J Biol Chem* 2000;**275**:9131–5
48. Neubauer K, Zieger B. The mammalian septin interactome. *Front Cell Dev Biol* 2017;**5**:3
49. Cao LQ, Shao ZL, Liang HH, Zhang DW, Yang XW, Jiang XF, Xue P. Activation of peroxisome proliferator-activated receptor-γ (PPARγ) inhibits hepatoma cell growth via downregulation of SEPT2 expression. *Cancer Lett* 2015;**359**:127–35
50. Koch M, Bohrmann B, Matthison M, Hagios C, Trueb B, Chiquet M. Large and small splice variants of collagen XII: differential expression and ligand binding. *J Cell Biol* 1995;**130**:1005–14
51. Kloeckener-Gruissem B, Neidhardt J, Magyar I, Plauchu H, Zech JC, Morlé L, Palmer-Smith SM, Macdonald MJ, Nas V, Fry AE, Berger W. Novel VCAN mutations and evidence for unbalanced alternative splicing in the pathogenesis of Wagner syndrome. *Eur J Hum Genet* 2013;**21**:352–6
52. Fang S, Huang Y, Zhong S, Li Y, Zhang Y, Li Y, Sun J, Liu X, Wang Y, Zhang S, Xu T, Sun X, Gu P, Li D, Zhou H, Li B, Fan X. Regulation of orbital fibrosis and adipogenesis by pathogenic Th17cCells in Graves orbitopathy. *J Clin Endocrinol Metab* 2017;**102**:4273–83
53. Ueno T, Fujimori K. Novel suppression mechanism operating in early phase of adipogenesis by positive feedback loop for enhancement of cyclooxygenase-2 expression through prostaglandin F2α receptor mediated activation of MEK/ERK-CREB Cascade. *FEBS J* 2011;**278**:2901–12
54. Khong JJ, Wang LY, Smyth GK, McNab AA, Hardy TG, Selva D, Llamas B, Jung CH, Sharma S, Burdon KP, Ebeling PR, Craig JE. Differential gene expression profiling of orbital adipose tissue in thyroid orbitopathy. *Invest Ophthalmol Vis Sci* 2015;**56**:6438–47

(Received January 29, 2021, Accepted April 16, 2021)